Inorg. Chem. **2003**, *42*, 7106–7115

Structural Studies on the Stepwise Chelating Processes of Bidentate 2-(Aminomethyl)pyridine and Tridentate Bis(2-pyridylmethyl)amine toward an Acetate-Bridged Dirhodium(II) Center

Takashi Yoshimura,[†] Keisuke Umakoshi,[‡] and Yoichi Sasaki*[,§]

Department of Chemistry, Graduate School of Science, Osaka University, Toyonaka, Osaka 560-0043, Japan, Department of Applied Chemistry, Faculty of Engineering, Nagasaki University, Bunkyo-machi, Nagasaki 852-8521, Japan, and Division of Chemistry, Graduate School of Science, Hokkaido University, Kita-ku, Sapporo 060-0810, Japan

Received March 13, 2003

Several intermediates and final products of the reactions of $[Rh_2(\mu\text{-}CH_3COO)_4(CH_3OH)_2]$ with a tridentate ligand bis(2-pyridylmethyl)amine (bpa) and bidentate 2-(aminomethyl)pyridine (amp) have been isolated, and the chelation processes of these ligands to the dirhodium(II) center are discussed. The reaction of a 2 equiv amount of bpa in chloroform afforded three products, $[Rh_2(\mu\text{-}CH_3COO)_2(\eta^1\text{-}CH_3COO)(bpa)_2]^+$ ([**1**]$^+$), *C*$_2$-$[Rh_2(\mu\text{-}CH_3COO)_2(bpa)_2]^{2+}$ ([**2a**]$^{2+}$), and *C*$_s$-$[Rh_2(\mu\text{-}CH_3COO)_2(bpa)_2]^{2+}$ ([**2b**]$^{2+}$), where *C*$_2$ and *C*$_s$ denote the molecular symmetry of the two geometrical isomers. X-ray crystallography revealed that [**1**]$^+$ contains *ax-eq* chelated bidentate and *ax-eq-eq* tridentate bpa and that [**2a**]$^{2+}$ and [**2b**]$^{2+}$ have two *ax-eq-eq* tridentate bpa ligands (*ax* denotes the site trans to the Rh–Rh bond, and *eq*, the site perpendicular to it). The reaction is initiated by almost instantaneous monodentate or inter-Rh_2-unit bridging coordination of bpa at the *ax* sites, which is followed by very slow *ax-eq* chelate formation and then ultimate *ax-eq-eq* tridentate coordination. The reaction of $[Rh_2(\mu\text{-}CH_3COO)_4(CH_3OH)_2]$ with amp in 1:2 ratio in chloroform initially gives an insoluble polymer in which amp interconnects the *ax* sites of the dirhodium(II) units. Further reactions afforded $[Rh_2(\mu\text{-}CH_3COO)_2(\eta^1\text{-}CH_3COO)(amp)_2]^+$ ([**4**]$^+$) and $[Rh_2(\mu\text{-}CH_3COO)_2(amp)_2]^{2+}$ ([**5**]$^{2+}$). The X-ray structural studies show that [**4**]$^+$ has one *ax-eq* and one *eq-eq* chelate and [**5**]$^{2+}$ two *eq-eq* chelates. More rigid tridentate ligands 2,2′:6′,2”-terpyridine (tpy) and 4′-chloro-2,2′:6′,2”-terpyridine (Cl-tpy) have been introduced at *ax* sites in a monodentate mode ($[Rh_2(\mu\text{-}CH_3COO)_4(tpy)_2]$ (**8**) and $[Rh_2(\mu\text{-}CH_3COO)_4(Cl\text{-}tpy)_2]$ (**9**)). While the Rh–Rh distances of these complexes and $[Rh_2(\mu\text{-}CH_3COO)_2(2,2'\text{-bipyridine})_2(py)_2]^{2+}$ ([**7**]$^{2+}$) are practically unchanged (2.56–2.60 Å) except for **8** and **9** (2.4 Å), the Rh–N_{ax} distances range from 2.11 to 2.35 Å. Relatively short distances are found for the compounds with *ax-eq* or *ax-eq-eq* chelates (<2.22 Å). Longest distances (2.32–2.35 Å) found for **8** and **9** may be due to the steric effect. The distances of other complexes fall in the normal region. The visible band of the $\pi^*_{Rh-Rh} \rightarrow \sigma^*_{Rh-Rh}$ transition in solid-state reflectance spectra shows a red-shift as the Rh–N_{ax} distances becomes longer.

Introduction

Dinuclear metal complexes where two metal centers are bridged by one to four carboxylate and analogous ligands take a range of single to quadruple metal-to-metal bonds depending on the number of d electrons.[1] While d^4 metal ions such as Mo(II) and Re(III) form the highest quadruple bonds, d^7 metal ions such as Rh(II) give a single bond.[2,3] The dinuclear complexes having these structural units receive continuous attention as they are quite stable and can be used to construct various new derivatives including supramolecular assemblies.[4−23] Substitution of the bridging ligands has been

* To whom correspondence should be addressed. E-mail: ysasaki@sci.hokudai.ac.jp.
[†] Osaka University.
[‡] Nagasaki University.
[§] Hokkaido University.

(1) Cotton, F. A.; Walton, R. A. *Multiple Bonds Between Metal Atoms*, 2nd ed.; Clarendon Press: Oxford, U.K., 1993.
(2) Felthouse, T. R. *Prog. Inorg. Chem.* **1982**, *29*, 73−166.
(3) Boyar, E. B.; Robinson, S. D. *Coord. Chem. Rev.* **1983**, *50*, 109−208.
(4) Sorasaenee, K.; Galán-Mascarós, J. R.; Dunbar, K. R. *Inorg. Chem.* **2003**, *42*, 661−663.
(5) Cotton, F. A.; Hillard, E. A.; Liu, C. Y.; Murillo, C. A.; Wang, W.; Wang, X. *Inorg. Chim. Acta* **2002**, *337*, 233−246.

10.1021/ic030093w CCC: $25.00
Published on Web 10/04/2003

often an important strategy to gain access to such derivatives, but only limited information is available on the mechanisms and kinetic aspects of the substitution reactions.[24−30] The exchange reaction between free trifluoroacetate ions and the bridging ones in $[Mo_2(\mu\text{-}CF_3COO)_4]$ in acetonitrile proceeds rapidly on the time scale of ^{19}F NMR spectroscopy ($(1.1 \pm 0.1) \times 10^4$ s^{-1} at 25 °C).[25] It has been suggested that even faster coordination of trifluoroacetate at the axial (*ax*) site (trans to the Mo−Mo bond) precedes the exchange reaction.[25] On the contrary, stepwise substitution of trifluoroacetate for the acetate ligands in $[Rh_2(\mu\text{-}CH_3COO)_4(py)_2]$ in neat trifluoroacetic acid requires refluxing conditions to monitor.[24] The ligand substitution at the *ax* sites is quite rapid, however, as revealed by the study of the pyridine exchange reaction at the *ax* sites of $[Rh_2(\mu\text{-}CH_3COO)_4(py)_2]$ in H_2O (10^5−10^6 M^{-1} s^{-1} at 25 °C).[31] The different substitution lability at the *eq* sites is also seen in doubly carboxylate bridged complexes $[M_2(\mu\text{-}RCOO)_2(CH_3CN)_4]^{2+}$ (M = Mo, Rh). While the exchange of equatorial CH_3CN ligands of the dimolybdenum complex proceeds even at −45 °C in CD_3CN, the exchange half-life $t_{1/2}$ is ca. 4 h for the dirhodium complex at 100 °C.[26]

Substitution reactions of the bridging ligands should be of multistep nature, and the characterization of various intermediate species formed during the reaction course should be important to visualize the reaction pathways. Considering the substitution inert nature, the dirhodium(II) center is more appropriate for the investigation of the stepwise reactions on the dimetal centers. In fact, the reactions of tetrakis(carboxylato)dirhodium(II) complexes with bidentate ligands such as 2,2′-bipyridine (bpy) and 1,10-phenanthroline (phen)[32−44] gave both $[Rh_2(\mu\text{-}RCOO)_3(bpy)_2]^+$ and $[Rh_2(\mu\text{-}CH_3COO)_2(bpy)_2(CH_3CN)_2]^{2+}$, where the former contains the axial−equatorial (*ax-eq*) chelate and the latter the *eq-eq* one. The former is regarded as a precursor to the latter. On the contrary, only *eq-eq*-chelated $[Mo_2(\mu\text{-}RCOO)_2(bpy)_2]^{2+}$ (R = CF_3, CHF_2) was isolated in the case of the dimolybdenum(II) complexes.[45,46] It appears that the slow substitution of the *eq* sites of dirhodium(II) complexes makes possible the isolation of the stepwise substitution products. For the substitution of tridentate 2,2′:6′,2″-terpyridine (tpy), two complexes, $[Rh_2(\mu\text{-}RCOO)_4(tpy)_2]$ and $[Rh_2(\mu\text{-}RCOO)(tpy)_2]^{3+}$, have been isolated.[43,47,48] In the former complex the tpy ligands coordinate as a monodentate ligand to the *ax* sites, while in the latter as a tridentate chelate at three *eq* sites of each metal center. The *ax-eq*-chelated intermediate species may be unstable due to steric rigidity of the tpy ligand. Facile coordination of the third pyridyl group would follow the formation of the *ax-eq*-chelated intermediate. Thus the characterization of the intermediate species for the substitution of tridentate ligands is restricted as far as the rigid ligands are employed.

It is interesting to investigate the reactivity of stereochemically more flexible di- and tridentate ligands such as 2-(pyridylmethyl)amine (amp) and bis(2-pyridylmethyl)amine (bpa) toward the carboxylate-bridged dirhodium(II) centers. Previously, it was reported that the reaction of amp

(6) Cotton, F. A.; Lin, C.; Murillo, C. A. *Acc. Chem. Res.* **2001**, *34*, 759−771.
(7) Cotton, F. A.; Hillard, E. A.; Murillo, C. A. *J. Am. Chem. Soc.* **2002**, *124*, 5658−5660.
(8) Miyasaka, H.; Campos-Fernández, C. S.; Clérac, R.; Dunbar, K. R. *Angew. Chem., Int. Ed.* **2000**, *39*, 3831−3835.
(9) Campos-Fernández, C. S.; Thomson, L. M.; Galán-Mascarós, J. R.; Ouyang, X.; Dunbar, K. R. *Inorg. Chem.* **2002**, *41*, 1523−1533.
(10) Cotton, F. A.; Lin, C.; Murillo, C. A. *Chem. Commun.* **2001**, 11−12.
(11) Cotton, F. A.; Lin, C.; Murillo, C. A. *J. Chem. Soc., Dalton Trans.* **2001**, 499−501.
(12) Sorasaenee, K.; Galán-Mascarós, J. R.; Dunbar, K. R. *Inorg. Chem.* **2002**, *41*, 433−436.
(13) Deubel, D. V. *Organometallics* **2002**, *21*, 4303−4305.
(14) Cotton, F. A.; Daniels, L. M.; Lin, C.; Murillo, C. A.; Yu, S.-Y. *J. Chem. Soc., Dalton Trans.* **2001**, 502−504.
(15) Cotton, F. A.; Dikarev, E. V.; Petrukhina, M. A. *J. Chem. Soc., Dalton Trans.* **2000**, 4241−4243.
(16) Cotton, F. A.; Dikarev, E. V.; Petrukhina, M. A.; Schmitz, M.; Stang, P. J. *Inorg. Chem.* **2002**, *41*, 2903−2908.
(17) Cotton, F. A.; Dikarev, E. V.; Petrukhina, M. A.; Stiriba, S.-E. *Polyhedron* **2000**, *19*, 1829−1835.
(18) Cotton, F. A.; Dikarev, E. V.; Petrukhina, M. A.; Stiriba, S.-E. *Organometallics* **2000**, *19*, 1402−1405.
(19) Cotton, F. A.; Dikarev, E. V.; Stiriba, S.-E. *Inorg. Chem.* **1999**, *38*, 4877−4881.
(20) Cotton, F. A.; Dikarev, E. V.; Stiriba, S.-E. *Organometallics* **1999**, *18*, 2724−2726.
(21) Cotton, F. A.; Lin, C.; Murillo, C. A. *Inorg. Chem.* **2001**, *40*, 5886−5889.
(22) Cotton, F. A.; Murillo, C. A.; Stiriba, S.-E. *Inorg. Chem. Commun.* **1999**, *2*, 463−464.
(23) Kawamura, T.; Maeda, M.; Miyamoto, M.; Usami, H.; Imaeda, K.; Ebihara, M. *J. Am. Chem. Soc.* **1998**, *120*, 8136−8142.
(24) Bear, J. L.; Kitchens, J.; Willcott, M. R., III *J. Inorg. Nucl. Chem.* **1971**, *33*, 3479−3486.
(25) Teramoto, K.; Sasaki, Y.; Migita, K.; Iwaizumi, M.; Saito, K. *Bull. Chem. Soc. Jpn.* **1979**, *52*, 446−452.
(26) Casas, J. M.; Cayton, R. H.; Chisholm, M. H. *Inorg. Chem.* **1991**, *30*, 358−360.
(27) Chisholm, M. H.; Huffman, J. C.; Iyer, S. S. *J. Chem. Soc., Dalton Trans.* **2000**, 1483−1489.
(28) Tresoldi, G.; De Munno, G.; Nicolo, F.; Lo Schiavo, S.; Piraino, P. *Inorg. Chem.* **1996**, *35*, 1377−1381.
(29) Lahuerta, P.; Paya, J.; Pellinghelli, M. A.; Tripicchio, A. *Inorg. Chem.* **1992**, *31*, 1224.
(30) Chisholm, M. H.; Macintosh, A. M. *J. Chem. Soc., Dalton Trans.* **1999**, 1205.
(31) Das, K.; Simmons, E. L.; Bear, J. L. *Inorg. Chem.* **1977**, *16*, 1268−1271.
(32) Pruchnik, F. P.; Jakimowicz, P.; Ciunik, Z. *Inorg. Chem. Commun.* **2001**, *4*, 726−729.
(33) Pruchnik, F. P.; Jakimowicz, P.; Ciunik, Z.; Stanislawek, K.; Oro, L. A.; Tejel, C.; Ciriano, M. A. *Inorg. Chem. Commun.* **2001**, *4*, 19−22.
(34) Galdecka, E.; Galdecki, Z.; Pruchnik, F. P.; Jakimowicz, P. *Transition Met. Chem.* **2000**, *25*, 315−319.
(35) Natkaniec, L.; Pruchnik, F. P. *J. Chem. Soc., Dalton Trans.* **1994**, 3261−3266.
(36) Szymaszek, A.; Pruchnik, F. P. *Pol. J. Chem.* **1992**, *66*, 1859−1865.
(37) Glowiak, T.; Pruchnik, F. P.; Zuber, M. *Pol. J. Chem.* **1991**, *65*, 1749−1754.
(38) Pruchnik, F. P. *Pure Appl. Chem.* **1989**, *61*, 795−804.
(39) Glowiak, T.; Pasternak, H.; Pruchnik, F. P. *Acta Crystallogr.* **1987**, *C43*, 1036−1038.
(40) Pruchnik, F. P.; Zuber, M. *Rocz. Chem.* **1977**, *51*, 1813−1819.
(41) Crawford, C. A.; Matonic, J. H.; Streib, W. E.; Huffman, J. C.; Dunbar, K. R.; Christou, G. *Inorg. Chem.* **1993**, *32*, 3125−3133.
(42) Lo Schiavo, S.; Sinicropi, M. S.; Tresoldi, G.; Arena, C. G.; Piraino, P. *J. Chem. Soc., Dalton Trans.* **1994**, 1517−1522.
(43) Crawford, C. A.; Matonic, J. H.; Huffman, J. C.; Folting, K.; Dunbar, K. R.; Christou, G. *Inorg. Chem.* **1997**, *36*, 2361−2371.
(44) Daniels, M. A. M.; Mehmet, N.; Tocher, D. A. *J. Chem. Soc., Dalton Trans.* **1991**, 2601−2606.
(45) Matonic, J. H.; Chen, S. J.; Perlepes, S. P.; Dunbar, K. R.; Christou, G. *J. Am. Chem. Soc.* **1991**, *113*, 8169−8171.
(46) Day, E. F.; Huffman, J. C.; Folting, K.; Christou, G. *J. Chem. Soc., Dalton Trans.* **1997**, 2837−2841.
(47) Pruchnik, F. P.; Robert, F.; Jeannin, Y.; Jeannin, S. *Inorg. Chem.* **1996**, *35*, 4261−4263.
(48) Bera, J. K.; Campos-Fernández, C. S.; Clérac, R.; Dunbar, K. R. *Chem. Commun.* **2002**, 2536−2537.

with $[Rh_2(\mu\text{-}CH_3COO)_4(CH_3OH)_2]$ in a 1:1 ratio gave an insoluble one-dimensional pink polymer, $[Rh_2(\mu\text{-}CH_3COO)_4(amp)]_n$, without substitution of the bridging acetate ligands.[49] In our preliminary account on the same reaction in 2:1 ratio (in ligand excess), however, we reported the isolation of discrete complexes with a different coordination mode of amp, $[Rh_2(\mu\text{-}CH_3COO)_2(\eta^1\text{-}CH_3COO)(amp)_2]ClO_4$ ([**4**]ClO_4) (*ax-eq* and *eq-eq* chelates), $[Rh_2(\mu\text{-}CH_3COO)_2(amp)_2](ClO_4)_2$ ([**5**]$(ClO_4)_2$) (*eq-eq* chelates), and $[Rh_2(\mu\text{-}CH_3COO)_2(amp)_2(py)_2](PF_6)_2$ ([**6**]$(PF_6)_2$) (*eq-eq* chelates).[50] Also, the rate of interconversion from *ax-eq* to *eq-eq*, namely from $[\mathbf{4}]^+$ to $[\mathbf{5}]^{2+}$, has been measured ($(2.5 \pm 0.1) \times 10^{-4}$ s^{-1} ($I = 0.075$ M ($LiClO_4$), pH = 6.5) at 75 °C).[50] The result quantitatively proved the substitution-inert nature of the *eq* sites of the dimeric rhodium(II) center. In this paper, we wish to report on the products of the reaction of bpa with $[Rh_2(\mu\text{-}CH_3COO)_4(CH_3OH)_2]$, together with the details on the study of the reaction of amp. When the above-mentioned tpy complexes of dirhodium(II) were published,[43] we had also been studying similar reactions independently to investigate the steric requirement of the tridentate ligand. Some of our relevant results on the reaction with tpy and its analogue 4-chloro-2,2′:6′,2″-terpyridine (Cl-tpy) are also included in this paper.

Experimental Section

Preparation of the Complexes. $[Rh_2(\mu\text{-}CH_3COO)_4(CH_3OH)_2]$[51] and bis(2-pyridylmethyl)amine[52] were prepared as described in the literature. All manipulations were performed under aerobic conditions.

$[Rh_2(\mu\text{-}CH_3COO)_2(\eta^1\text{-}CH_3COO)(bpa)_2]PF_6$ ([1]PF_6) and $[Rh_2(\mu\text{-}CH_3COO)_2(bpa)_2](PF_6)_2$ (C_2 Isomer, [2a]$(PF_6)_2$; C_s Isomer [2b]$(PF_6)_2$). Two geometrical isomers have been obtained for $[Rh_2(\mu\text{-}CH_3COO)_2(bpa)_2]^{2+}$. They are abbreviated as C_2 and C_s isomers by considering their molecular symmetry (vide infra).

A chloroform solution (10 mL) of bpa (155 mg, 0.8 mmol) was added to a suspension of $[Rh_2(\mu\text{-}CH_3COO)_4(CH_3OH)_2]$ (200 mg, 0.4 mmol) in 30 mL of chloroform. The complex quickly dissolved to give a clear solution, the color of which changed immediately from green to purple. The solution was continuously stirred at 20 °C for 6 d, during which time the color of the solution further changed to orange. The solvent was then evaporated to dryness, and the residue was dissolved in 150 mL of water. The orange solution was poured onto a cation-exchange column of SP-Sephadex C-25 (Na^+ form, 2.5 × 30 cm). An orange band was held at the top of the column. The first band was eluted with aqueous 0.05 M NaCl solution. To the eluate was added an aqueous solution (10 mL) of 1.0 g of NH_4PF_6. The solution was allowed to stand for several days. The resulting orange-red microcrystals of [**1**]$PF_6 \cdot 1.5H_2O$ were filtered out, washed with a small amount of water, and then dried in air. Yield: 49 mg (13%). Anal. Calcd for $C_{30}H_{37}F_6N_6O_{7.5}PRh_2$: C, 37.79; H, 4.02; N, 8.81. Found: C, 37.85; H, 3.78; N, 8.82. Recrystallization from a mixed solvent of methanol/water (1/1 v/v) gave crystals suitable for X-ray structural analysis. ^{1}H NMR (270 MHz, $CDCl_3$, TMS)/δ (ppm): acetate, 1.00 (3H, s), 1.81 (3H, s), 2.43 (3H, s); bpa $-CH_2-$, 3.33 (1H, dd), 3.41 (1H, d), 3.70 (1H, d), 4.00 (1H, dd), 4.31 (1H,d), 4.43 (1H, d), 4.70 (1H, d), 5.36 (1H, dd); bpa aromatic rings, 6.97 (1H, dd), 7.12 (1H, d), 7.37 (1H, dd), 7.50 (2H, m), 7.56 (1H, d), 7.61 (1H, dd), 7.79 (1H, dd), 7.82 (3H, d), 7.89(1H, dd) 7.95 (1H, dd), 8.75 (1H, d), 9.05 (1H, d), 9.37 (2H, d). UV−vis/nm (ϵ/M^{-1} cm^{-1}): in CH_2Cl_2, 486 (410), 295 (22 400); in CH_3CN, 494 (460), 296 (26 200), 254 (15 400).

The second band was eluted with aqueous 0.15 M NaCl solution. To the eluate was added an aqueous solution (10 mL) of 1.0 g of NH_4PF_6. The orange solid of [**2a**]$(PF_6)_2$ precipitated immediately, which was filtered out, washed with water, and then dried in air. Yield: 146 mg (36%). Anal. Calcd for $C_{28}H_{32}F_{12}N_6O_4P_2Rh_2$: C, 33.22; H, 3.19; N, 8.30. Found: C, 32.99; H, 3.24; N, 8.23. ^{1}H NMR (270 MHz, CD_2Cl_2, TMS)/δ (ppm): acetate, 2.26 (6H, s); bpa $-CH_2-$, 2.56 (2H, dd), 3.56 (2H, d), 4.06 (2H, d), 4.68 (2H, dd); bpa $-NH-$, 4.82 (2H, br); bpa aromatic rings, 6.89 (2H, d), 7.46 (4H, m), 7.55 (2H, dd), 7.69 (2H, dd), 7.85 (2H, dd), 8.76 (2H, d), 8.98 (2H, d). UV−vis/nm (ϵ/M^{-1} cm^{-1}): in CH_2Cl_2, 456 (710), 325 (sh), 287 (28 300); in CH_3CN, 458 (650), 326 (sh), 285 (28 000), 248 (15 000); in the solid state, 454. Recrystallization from methanol gave crystals suitable for X-ray structural analysis.

The third band was eluted also with 0.15 M NaCl solution. To the eluate was added an aqueous solution (10 mL) of 1.0 g of NH_4PF_6. The orange solid of [**2b**]$(PF_6)_2$ was precipitated immediately, which was filtered out, washed with water, and then dried in air. Yield: 47 mg (11%). Anal. Calcd for $C_{28}H_{32}F_{12}N_6O_4P_2Rh_2 \cdot 4H_2O$: C, 31.01; H, 3.72; N, 7.75. Found: C, 30.60; H, 3.20; N, 7.98. ^{1}H NMR (CD_2Cl_2, TMS)/δ (ppm): acetate, 1.98 (3H, s), 2.55 (3H, s); bpa $-CH_2-$, 3.97 (2H, d), 4.26 (2H, d), 4.59 (2H, dd), 4.77 (2H, dd); bpa $-NH-$, 6.68 (2H, br); bpa aromatic rings, 6.86 (2H, d), 6.98 (2H, dd), 7.34 (2H, dd), 7.47 (2H, dd), 7.57 (2H, d), 7.91 (4H, m), 8.88 (2H, d). UV−vis/nm (ϵ/M^{-1} cm^{-1}): in CH_2Cl_2, 467 (560), 295 (26 100); in CH_3CN, 467 (580), 292 (28 700). The single crystals for X-ray analysis were obtained as the BF_4^- salt, [**2b**]$(BF_4)_2$, by the addition of an aqueous solution of NH_4BF_4 to the eluate.

$[\{Rh_2(\mu\text{-}CH_3COO)_4\}_3(bpa)_2]_n$ (3). A methanol solution (10 mL) of bpa (16 mg, 0.08 mmol) was added to that (20 mL) of $[Rh_2(\mu\text{-}CH_3COO)_4(CH_3OH)_2]$ (21 mg, 0.04 mmol). The clear solution was stirred at 20 °C. The solution immediately turned to purple in color, from which a pink solid separated out within 5 min. After further stirring for 1 h, the pink solid was filtered out, washed with methanol, and then dried in vacuo. Yield of **3**: 18 mg (76%). Anal. Calcd for $C_{48}H_{88}N_6O_{24}Rh_6$: C, 33.43; H, 3.62; N, 4.87. Found: C, 33.16; H, 3.61; N, 5.13. When the reaction was

(49) Crawford, C. A.; Day, E. F.; Streib, W. E.; Huffman, J. C.; Christou, G. *Polyhedron* **1994**, *13*, 2933−2943.
(50) Yoshimura, T.; Umakoshi, K.; Sasaki, Y. *Chem. Lett.* **1999**, 267−268.
(51) Rempel, G. A.; Legzdins, P.; Smith, H.; Wilkinson, G. *Inorg. Synth.* **1972**, *13*, 90−91.
(52) Sugimoto, H.; Matsunami, C.; Koshi, C.; Yamasaki, M.; Umakoshi, K.; Sasaki, Y. *Bull. Chem. Soc. Jpn.* **2001**, *74*, 2091−2099.

carried out in the 1:1 ratio (0.060 mmol each) in methanol (40 mL), similar pink precipitate was obtained within a few minutes after the mixing. The elemental analyses (C, 33.51; H, 3.55; N, 5.12) of the product are again consistent with the 3:2 ratio of the dimeric unit to the ligand.

$[Rh_2(\mu\text{-}CH_3COO)_2(\eta^1\text{-}CH_3COO)(amp)_2]ClO_4$ ([4]ClO_4) and $[Rh_2(\mu\text{-}CH_3COO)_2(amp)_2](ClO_4)_2$ ([5]$(ClO_4)_2$). A chloroform solution (10 mL) of amp (64 mg, 0.6 mmol) was added to that (100 mL) of $[Rh_2(\mu\text{-}CH_3COO)_4(CH_3OH)_2]$ (200 mg, 0.4 mmol). While the clear solution was stirred at 20 °C, its color changed immediately from green to purple, and pink solid appeared after 15 min. The suspension was continuously stirred for 3 d to give clear purple solution. The solvent was removed, and the residue was dissolved into 10 mL of water. To this aqueous solution was added an aqueous solution (10 mL) of $NaClO_4 \cdot H_2O$ (300 mg, 2.13 mmol), and the mixture was allowed to stand for several days, during which time purple crystals appeared. The crystals of [**4**]ClO_4 were collected and washed with small amount of water and dried in air. Yield: 111 mg (40%). Anal. Calcd for $C_{18}H_{25}N_4O_{10}ClRh_2$: C, 30.94; H, 3.61, N, 8.02. Found: C, 29.83; H, 3.64; N 7.96. ^{1}H NMR (270 MHz, D_2O, DSS)/δ (ppm): acetate, 1.72 (3H, s), 2.02 (3H, s), 2.26 (3H, s); amp $-CH_2-$, 4.01 (3H, m), 4.30 (1H, m); amp $-NH_2-$, 3.80 (1H, br), 4.50 (1H, br), 4.94 (1H, br), 6.25 (1H, br); amp aromatic rings, 7.38 (1H, dd), 7.42 (1H, d), 7.54 (1H, d), 7.62 (1H, dd), 7.91 (1H, dd), 8.02 (1H, dd), 8.32 (1H, d), 8.96 (1H, d). UV−vis/nm (ϵ/M^{-1} cm^{-1} in H_2O): 536 (220), 311 (8700), 274 (18 300).

The filtrate was allowed to evaporate slowly to give a green microcrystalline solid, which was collected, washed several times with small amount of water, and then dried in vacuo. Yield of [**5**]$(ClO_4)_2$: 20 mg (6.5%). Anal. Calcd for $C_{16}H_{22}N_4O_{12}Cl_2Rh_2$: C, 26.00; H, 3.00; N, 7.58; Cl, 9.59. Found: C, 26.22; H, 3.16; N, 7.56; Cl, 9.37. FAB-MS (M^+): *m*/*z* 639. ^{1}H NMR (270 MHz, D_2O, DSS)/δ (ppm): acetate, 2.26 (6H, s); amp $-CH_2-$, 2.0 (2H, dd), 3.88 (2H, d); amp $-NH_2$, 4.11 (2H, br); amp aromatic rings, 7.32 (2H, d), 7.54 (2H, dd), 7.97 (2H, dd), 8.57 (2H, d). UV−vis/nm (ϵ/M^{-1} cm^{-1} in H_2O): 577 (150), 310 (8500), 266 (16 900). The chloride salt of [**5**]Cl_2 (yield 76 mg, 29%) was prepared by the similar method except for dissolving the residue into an aqueous solution (15 mL) of sodium chloride (500 mg, 8.5 mmol) instead of an aqueous solution of $NaClO_4 \cdot H_2O$.

$[Rh_2(\mu\text{-}CH_3COO)_2(amp)_2(py)_2](PF_6)_2$ ([6]$(PF_6)_2$). Pyridine (50 μL, 0.62 mmol) was added to an aqueous solution (10 mL) of [**5**]Cl_2 (25 mg, 0.04 mmol) with stirring at 20 °C. The color of the solution changed immediately from green to pink. After 1 h an aqueous solution (10 mL) of NH_4PF_6 (200 mg, 1.23 mmol) was added to the reaction mixture to give a pink solid, which was filtered off, washed several times with a small amount of water, and dried in vacuo. Yield: 27 mg (70%). Anal. Calcd for $C_{26}H_{32}F_{12}N_6O_4P_2Rh_2$: C, 31.60; H, 3.26; N, 8.50. Found: C, 31.45; H, 3.25; N, 8.73. ^{1}H NMR (270 MHz, CD_2Cl_2, TMS)/δ (ppm): acetate, 2.23 (6H, s); amp $-CH_2-$, 2.25 (2H, d), 3.85 (2H, d); amp $-NH_2$, 3.50 (2H, br); amp aromatic rings, 7.19 (2H, d), 7.70 (2H, dd), 7.95 (2H, dd), 8.68 (2H, d); pyridine, 7.50 (4H, dd), 7.92 (2H, dd), 8.38 (4H, d). UV−vis/nm (ϵ/M^{-1} cm^{-1}): in CH_2Cl_2, 495 (450), 310 (sh), 288 (28 500); in CH_3CN, 530 (250), 340 (sh), 285 (28 000), 267 (20 000); in the solid state, 508. Recrystallization from methanol gave crystals suitable for X-ray structural analysis.

$[Rh_2(\mu\text{-}CH_3COO)_2(bpy)_2(py)_2](PF_6)_2$ ([7]$(PF_6)_2$). To a methanol solution (50 mL) of $[Rh_2(\mu\text{-}CH_3COO)_4(CH_3OH)_2]$ (100 mg, 0.2 mmol) and 2,2′-bipyridine (62 mg, 0.4 mmol) was added a methanol solution of 0.12 M of HCl (3.3 mL, 0.4 mmol), and the mixture was refluxed for 1 h. The color of the solution changed from green to brown within 5 min. The volume of the solution was then reduced to 20 mL, and the solution was allowed to stand for 1 d in a refrigerator. Brown microcrystalline solid ($[Rh_2(\mu\text{-}CH_3COO)_2(bpy)_2Cl_2]$) was filtered off, washed with a small amount of methanol, and dried in vacuo.

To an aqueous solution (10 mL) of $[Rh_2(\mu\text{-}CH_3COO)_2(bpy)_2Cl_2]$ (50 mg, 0.083 mmol) was added pyridine (50 μL, 0.62 mmol), and the mixture was stirred at 20 °C for 1 h. The color of the solution changed from brown to orange. Addition of an aqueous solution (10 mL) of NH_4PF_6 (200 mg, 1.23 mmol) gave an orange precipitate, which was filtered off, washed several times with a small amount of water, and dried in vacuo. Yield: 54 mg (66% based on $[Rh_2(\mu\text{-}CH_3COO)_2(bpy)_2Cl_2]$). Anal. Calcd for $C_{34}H_{32}F_{12}N_6O_4P_2Rh_2$: C, 37.66; H, 2.97; N, 7.75. Found: C, 37.09; H, 2.90; N, 8.12. ^{1}H NMR (270 MHz, CD_2Cl_2, TMS)/δ (ppm): acetate, 2.53 (6H, s); bpy and py, 7.32 (4H, dd), 7.38 (4H, dd), 7.79 (2H, dd), 7.88 (2H, m), 7.97 (4H, d), 8.30 (4H, d). UV−vis/nm (ϵ/M^{-1} cm^{-1} in CH_3CN): 411 (3200), 348 (7100), 268 (41 500), 253 (48 300), 223 (45 000). Single crystals suitable for X-ray structural analysis were obtained by slow evaporation of the filtrate.

$[Rh_2(\mu\text{-}CH_3COO)_4(tpy)_2]$ (8). An acetone solution (20 mL) of an excess amount of tpy (93 mg, 0.4 mmol) was mixed with that (50 mL) of $[Rh_2(\mu\text{-}CH_3COO)_4(CH_3OH)_2]$ (50 mg, 0.1 mmol). Slow evaporation of the reaction mixture gave purple crystals, which were collected, washed with ether, and dried in air. Yield: 80 mg (89%). Anal. Calcd for $C_{38}H_{34}N_6O_8Rh_2$: C, 50.24; H, 3.77; N, 9.25. Found: C, 50.28; H, 3.82; N, 9.39. UV−vis/nm (in the solid state): 561.

$[Rh_2(\mu\text{-}CH_3COO)_4(Cl\text{-}tpy)_2]$ (9). A methanol solution (40 mL) of an excess amount of Cl-tpy (107 mg, 0.4 mmol) was mixed with that (50 mL) of $[Rh_2(\mu\text{-}CH_3COO)_4(CH_3OH)_2]$ (50 mg, 0.1 mmol). Slow evaporation of the reaction mixture gave purple crystals, which were collected, washed with dichloromethane, and dried in air. Yield: 79 mg (82%). Anal. Calcd for $C_{38}H_{32}Cl_2N_6O_8Rh_2$: C, 46.70; H, 3.30; N, 8.60; Cl, 7.25. Found: C, 46.64; H, 3.18; N, 8.62; Cl, 7.31. UV−vis/nm (in the solid state): 561.

Crystallographic Studies. The crystals of [**2a**]$(PF_6)_2$, [**2b**]$(BF_4)_2$, **8**, and **9** were mounted on a glass fiber, while those of [**1**]$PF_6 \cdot 1.5H_2O$ and [**7**]$(PF_6)_2 \cdot 0.5CH_3OH$ were sealed in a thin-walled glass capillary. The data for [**2a**]$(PF_6)_2$, [**2b**]$(BF_4)_2$, and **8** were collected on a MacScience MXC18, and those for [**7**]$(PF_6)_2 \cdot 0.5CH_3OH$ and **9** on a Rigaku AFC-5R diffractometer at 296 K. X-ray data for [**1**]$PF_6 \cdot 1.5H_2O$ were collected at ambient temperature on a Rigaku AFC-7S

Table 1. Crystallographic Data for $[Rh_2(\mu\text{-}CH_3COO)_2(\eta^1\text{-}CH_3COO)(bpa)_2]PF_6\cdot 1.5H_2O$ ([**1**]$PF_6\cdot 1.5H_2O$) C_2-$[Rh_2(\mu\text{-}CH_3COO)_2(bpa)_2](PF_6)_2$ ([**2a**]$(PF_6)_2$), (C_s-$[Rh_2(\mu\text{-}CH_3COO)_2(bpa)_2](BF_4)_2$ ([**2b**]$(BF_4)_2$), $[Rh_2(\mu\text{-}CH_3COO)_2(bpy)_2(py)_2](PF_6)_2\cdot 0.5CH_3OH$ ([**7**]$(PF_6)_2\cdot 0.5CH_3OH$), $[Rh_2(\mu\text{-}CH_3COO)_2(tpy)_2]$ (**8**), and $[Rh_2(\mu\text{-}CH_3COO)_2(Cl\text{-}tpy)_2]$ (**9**)

	[**1**]$PF_6\cdot 1.5H_2O$	[**2a**]$(PF_6)_2$	[**2b**]$(BF_4)_2$
formula	$C_{28}H_{35}F_{12}N_6O_{5.5}P_2Rh_2$	$C_{28}H_{32}F_{12}N_6O_4P_2Rh_2$	$C_{28}H_{32}B_2F_8N_2O_4Rh_2$
fw	953.44	1012.34	896.02
space group	$P\bar{1}$ (No. 2)	$P2_1/a$ (No. 14)	$P\bar{1}$ (No. 2)
a/Å	13.569(2)	25.974(9)	10.672(1)
b/Å	16.015(2)	12.469(4)	12.441(2)
c/Å	9.056(1)	11.288(3)	12.915(2)
α/deg	103.98(1)	90	80.55(1)
β/deg	101.025(10)	92.91(3)	82.25(1)
γ/deg	74.808(10)	90	88.41(1)
V/Å^3	1825.7(4)	3651(2)	1675.9(4)
Z	2	4	2
T/°C	25	−110	−90
λ/Å	0.710 69	0.710 73	0.710 73
d_{calcd}/g cm^{-3}	1.734	1.842	1.776
μ(Mo Kα)/cm^{-1}	10.31	10.78	10.55
R^a (R_w)^b	0.052 (0.098)	0.050 (0.064)	0.049 (0.064)

	[**7**]$(PF_6)_2\cdot 0.5CH_3OH$	**8**	**9**
formula	$C_{34.5}H_{34}F_{12}N_6O_{4.5}P_2Rh_2$	$C_{38}H_{34}N_6O_8Rh_2$	$C_{38}H_{32}Cl_2N_6O_8Rh_2$
fw	1100.43	908.53	977.42
space group	$P\bar{1}$ (No. 2)	$P\bar{1}$ (No. 2)	$P\bar{1}$ (No. 2)
a/Å	15.553(2)	10.043(2)	9.652(2)
b/Å	21.871(3)	13.433(3)	14.198(2)
c/Å	13.338(2)	8.012(2)	8.013(1)
α/deg	106.60(1)	104.83(2)	97.98(1)
β/deg	91.77(1)	94.64(1)	112.78(1)
γ/deg	87.07(1)	69.23(1)	72.63(1)
V/Å^3	4341(1)	976.9(3)	966.0(3)
Z	4	1	1
T/°C	23	23	23
λ/Å	0.710 69	0.710 73	0.710 69
d_{calcd}/g cm^{-3}	1.683	1.540	1.680
μ(Mo Kα)/cm^{-1}	9.29	8.86	10.38
R^a (R_w)^b	0.070 (0.081)	0.029 (0.037)	0.050 (0.059)

^{a} $\mathbf{P} = \Sigma||F_o| - |F_c||/\Sigma|F_o|$. ^{b} $R_w = [\Sigma w(|F_o| - |F_c|)^2/\Sigma w|F_o|^2]^{1/2}$.

diffractometer. Unit cell parameters of [**2a**]$(PF_6)_2$, [**2b**]$(BF_4)_2$, and **8** were obtained by least-squares refinement of 26 reflections ($25 \le 2\theta \le 35°$), while for those of [**1**]$PF_6\cdot 1.5H_2O$, [**7**]$(PF_6)_2\cdot 0.5CH_3OH$, and **9** 25 reflections ($25 \le 2\theta \le 30°$) were used. All data were corrected for Lorentz and polarization effects, and absorption corrections were applied for each data set.

The crystal structures of [**1**]$PF_6\cdot 1.5H_2O$, [**2b**]$(BF_4)_2$, [**6**]$(PF_6)_2$, **8**, and **9** were solved by direct method (SIR92),[53] while those of [**2a**]$(PF_6)_2$ and [**7**]$(PF_6)_2\cdot 0.5CH_3OH$ were solved by the heavy atom method (DIRDIF).[54] The positional and thermal parameters of non-hydrogen atoms were refined anisotropically by the full-matrix least-squares method. Hydrogen atoms were included at calculated positions with fixed displacement parameters (1.2 times the displacement parameters of the host atom).

Calculations were performed using CRYSTAN[55] for [**2a**]$(PF_6)_2$, [**2b**]$(BF_4)_2$, and **8** and TEXSAN[56] for [**1**]PF_6, [**7**]$(PF_6)_2\cdot 0.5CH_3OH$, and **9**. Further crystallographic data are given in Table 1. Listings of selected bond distances and angles are summarized in Table 2.

Other Measurements. The ^{1}H NMR spectra were obtained at 270 MHz with a JEOL JNM-EX270 spectrometer. ^{1}H chemical shifts were measured relative to the methyl resonance of TMS or DSS (for [**4**]ClO_4 and [**5**]$(ClO_4)_2$). UV−visible and reflectance spectra were recorded on a Hitachi U3410 spectrophotometer.

Results and Discussion

Stepwise Chelating Processes of the Bidentate and Tridentate Ligands toward the Dirhodium(II) Center. We have isolated several reaction products from the reaction mixture of $[Rh_2(\mu\text{-}CH_3COO)_4(CH_3OH)_2]$ with bidentate amp or tridentate bpa ligand. On the basis of the structures of these complexes (vide infra), the reaction pathways are summarized in Schemes 1 and 2 for the reactions of amp and bpa, respectively. Coordination of the chelating ligands may be initiated by rapid coordination at the *ax* sites. Because of the low solubility, polymeric species quickly precipitate where the chelating ligand (amp or bpa) acts as a bridge between the dimeric units. In the presence of an excessive amount of the ligand, the polymeric species could be in equilibrium with discrete species in solution in which the *ax* sites are occupied by the nonbridging monodentate amp or bpa. The discrete species then undergo very slow *ax-eq* chelate formation, followed by the *ax-eq* to *eq-eq* rearrange-

(53) Altomare, A.; Cascarano, G.; Giacovazzo, C.; Guagliardi, A.; Burla, M. C.; Polidori, G.; Camalli, M. *J. Appl. Crystallogr.* **1994**, *27*, 435.
(54) Beurskens, P. T.; Admiraal, G.; Beurskens, G.; Bosman, W. P.; Garcia-Granda, S.; Gould, R. O.; Smits, J. M. M. *DIRDIF*; Crystallography Laboratory, University of Nijmengen: Nijmengen, The Netherlands, 1992.
(55) Edwards, C.; Gilmore, C. J.; Mackay, S.; Stewart, N. *CRYSTAN*; MacScience: Yokohama, Japan, 1995.
(56) *TEXSAN*; Molecular Structure Corp.: The Woodlands, TX 77381, 1992.

Table 2. Selected Bond Lengths (Å) and Angles (deg) for $[Rh_2(\mu\text{-}CH_3COO)_2(\eta^1\text{-}CH_3COO)(bpa)_2]PF_6\cdot 1.5H_2O$ ([**1**]$PF_6\cdot 1.5H_2O$), C_2-$[Rh_2(\mu\text{-}CH_3COO)_2(bpa)_2](PF_6)_2$ ([**2a**]$(PF_6)_2$), C_s-$[Rh_2(\mu\text{-}CH_3COO)_2(bpa)_2](BF_4)_2$ ([**2b**]$(BF_4)_2$), $[Rh_2(\mu\text{-}CH_3COO)_2(bpy)_2(py)_2](PF_6)_2\cdot 0.5CH_3OH$ ([**7**]$(PF_6)_2\cdot 0.5CH_3OH$), $[Rh_2(\mu\text{-}CH_3COO)_4(tpy)_2]$ (**8**), and $[Rh_2(\mu\text{-}CH_3COO)_4(Cl\text{-}tpy)_2]$ (**9**)

	[**1**]$PF_6\cdot 1.5H_2O$	[**2a**]$(PF_6)_2$	[**2b**]$(BF_4)_2$
	Bond Lengths		
Rh···Rh	2.565(1)	2.568(1)	2.600(1)
Rh−O(bridging acetate)	2.040(7)−2.059(7)	2.039(6)−2.076(6)	2.042(3)−2.059(3)
av	2.056	2.053	2.050
Rh−O(monodentate)	2.047(7)		
Rh−N_{eq}(py)	2.008(8)	2.000(7), 2.000(7)	2.000(4), 2.007(3)
av		2.000	2.004
Rh−N(amine)	2.056(8), 2.069(8)	2.058(7), 2.061(7)	2.052(4), 2.054(4)
av	2.063	2.059	2.053
Rh−N_{ax}(py)	2.183(8), 2.253(8)	2.179(7), 2.198(7)	2.157(4), 2.203(4)
av	2.218	2.189	2.180
	Bond Angles		
Rh···Rh−O(bridging acetate)	84.4(2)−85.6(2)	84.2(2)−84.9(2)	83.9(1)−85.7(1)
av	84.9	84.5	84.6
Rh···Rh−O(monodentate acetate)	98.2(2)		
Rh···Rh−N_{eq}(py)	98.5(2)	100.4(2), 100.9(2)	96.2(1), 99.7(1)
av		100.7	98.0
Rh···Rh−N(amine)	101.3(2), 104.7(2)	102.1(2), 103.3(2)	105.3(1), 106.0(1)
av	103.0	102.7	105.7
Rh···Rh−N_{ax}(py)	172.6(2), 173.2(2)	172.5(2), 173.7(2)	170.7(1), 171.5(1)
av	172.9	173.1	171.1
	[**7**]$(PF_6)_2\cdot 0.5CH_3OH$	**8**	**9**
	Bond Lengths		
Rh···Rh	2.584(2), 2.593(2)	2.408(1)	2.405(1)
Rh−O(bridging acetate)	2.04(1)−2.069(9)	2.032(2)−2.048(2)	2.032(4)−2.046(4)
av	2.05	2.039	2.039
Rh−N_{eq}(py)	1.97(1)−2.00(1)		
av	1.98		
Rh−N_{ax}(py)	2.20(1)−2.27(1)	2.323(2)	2.359(6)
av	2.23		
	Bond Angles		
Rh···Rh−O(bridging acetate)	84.0(3)−85.4(3)	87.2(1)−88.4(1)	86.7(1)−88.5(1)
av	84.9	87.8	87.7
Rh···Rh−N_{eq}(py)	95.0(3)−99.3(3)		
av	97.3		
Rh···Rh−N_{ax}(py)	166.3(3)−169.0(4)	176.8(1)	174.2(1)
av	167.5		

Scheme 1

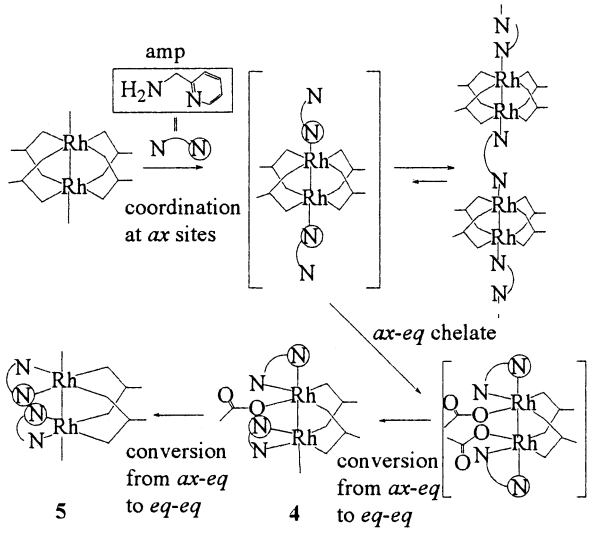

Scheme 2

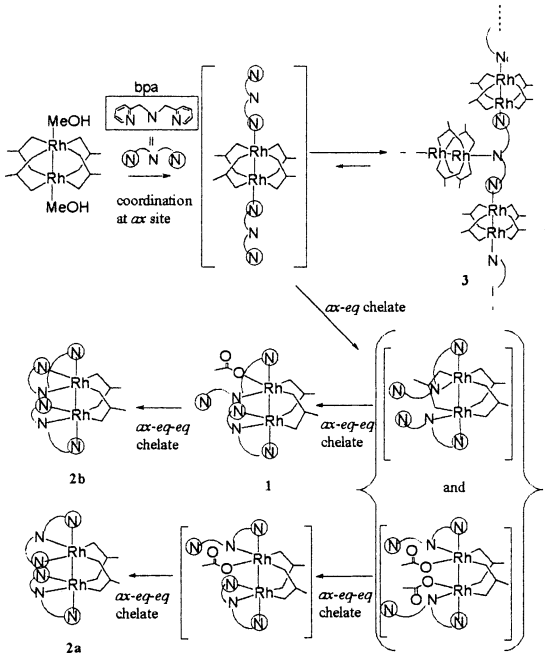

ment and/or further to *eq-eq* chelation (in the case of bpa). Further details are discussed below.

When the reaction of $[Rh_2(\mu\text{-}CH_3COO)_4(CH_3OH)_2]$ with amp is carried out by using 2 equiv of amp, the pink solid precipitated initially as in the case of the reaction in a 1:1 reactants ratio.[49] Further stirring of the suspension for 1 week afforded the soluble purple complex $[\mathbf{4}]^+$. It is possible that the discrete species, $[Rh_2(\mu\text{-}CH_3COO)_4(amp)_2]$, which may

be in equilibrium with the polymeric species, would undergo slow *ax-eq* chelation accompanied by the detachment of the bridging acetate. Successive rearrangement of one of the *ax-eq* chelate rings to the *eq-eq* mode affords the asymmetric complex cation $[\mathbf{4}]^+$. It was reported that the *eq-eq* chelating mode is thermally more stable.[26,41]

The rearrangement of the remaining *ax-eq* amp chelate of $[\mathbf{4}]^+$ to *eq-eq* mode took place at elevated temperature to give C_2 symmetric $[\mathbf{5}]^+$. Although the relative yield of $[\mathbf{5}]^+$ is rather low under the synthetic conditions, kinetic studies reported in our preliminary communication indicated almost complete conversion of $[\mathbf{4}]^+$ to $[\mathbf{5}]^+$. Kinetics parameters of the conversion were reported (the first-order rate constant in aqueous solution ($I = 0.075$ M ($LiClO_4$)), $(2.5 \pm 0.1) \times 10^{-4}$ s^{-1} at 75 °C ($\Delta H^{\ddagger} = 91 \pm 5$ kJ mol^{-1} and $\Delta S^{\ddagger} = -54 \pm 13$ J $K^{-1}mol^{-1}$)).[50] The C_2 symmetry of $[\mathbf{5}]^+$ was confirmed by ^1H NMR spectra (vide infra). A geometrical isomer with C_s symmetry is possible for $[\mathbf{5}]^+$, but the ^1H NMR spectra as well as the kinetic studies indicated the exclusive formation of $[\mathbf{5}]^+$ from $[\mathbf{4}]^+$. It is concluded that the conversion takes place stereoselectively, simply by the attack of *ax*-coordinated pyridyl nitrogen to expel the *eq*-coordinated monodentate acetate. The C_s isomer could be formed from the corresponding isomer of $[\mathbf{4}]^+$ in which the relative orientation of the *eq-eq* amp ligand is reversed. None of these isomers were isolated in this study or confirmed in the reaction mixture due to its complicated NMR spectra. Considering the relatively low yield of $[\mathbf{4}]^+$ and $[\mathbf{5}]^+$ (total yield, 46.5%), however, it is well possible that these isomers could be formed in the reaction mixture.

The reaction of $[Rh_2(\mu\text{-}CH_3COO)_4(CH_3OH)_2]$ with tridentate bpa in methanol also gave an insoluble pink solid, which was assigned as a polymer compound, $[\{Rh_2(\mu\text{-}CH_3COO)_4\}_3(bpa)_2]_n$. When the reaction was carried out in chloroform, no pink precipitate separated out, although the color of the reaction mixture turned purple immediately. It seems that the discrete species $[Rh_2(\mu\text{-}CH_3COO)_4(bpa)_2]$ may be predominant in chloroform. With samples being stirred for several days, further reactions proceeded as the purple solution ($\lambda_{max} = 534$ nm) turned to orange red (λ_{max} = ca. 460 nm). Three complexes have been separated by cation-exchange column chromatography. The asymmetric complex $[\mathbf{1}]^+$ contains two types of bpa, i.e., an *ax-eq* bidentate mode with a free pyridyl group and a full coordination (*ax-eq-eq*) mode. Complex cation $[\mathbf{1}]^+$ may be regarded as a precursor to $[\mathbf{2a}]^{2+}$ and/or $[\mathbf{2b}]^{2+}$, which have two fully coordinated bpa ligands. If the monodentate acetate ligand in $[\mathbf{1}]^+$ is directly replaced by the free pyridyl group of the bpa, the C_s isomer ($[\mathbf{2b}]^{2+}$) should be formed. An alternative mechanism is possible, i.e., the rearrangement of *ax*-pyridyl nitrogen to the *eq* site by expelling the monodentate acetate followed by the coordination of free pyridyl nitrogen to *ax* site. By this mechanism also, the C_s isomer is obtained. Therefore, $[\mathbf{1}]^+$ may be regarded as a precursor to $[\mathbf{2b}]^{2+}$. Since no isomerization between $[\mathbf{2a}]^{2+}$ and $[\mathbf{2b}]^{2+}$ was observed in solution, facial coordination is stable when once formed. The C_s isomer $[\mathbf{2a}]^{2+}$ should be formed from the unisolated isomer to $[\mathbf{1}]^+$ where the relative location of monodentate acetate and pyridyl donor sites at the two *eq* planes is different. Although the isomer was not isolated, it may be involved in the reaction mixture. The total yield of the three species (60%) is not very high even if the purification procedures are taken into account.

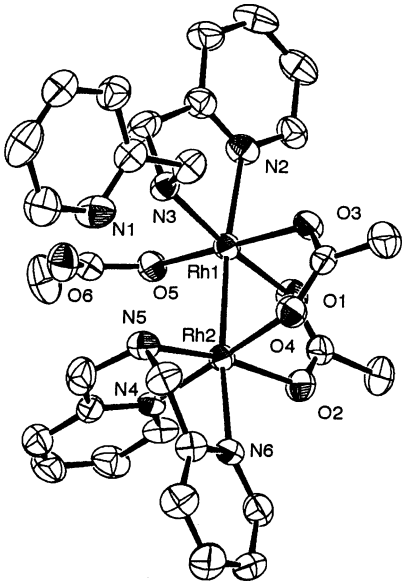

Figure 1. ORTEP drawing of $[Rh_2(\mu\text{-}CH_3COO)_2(\eta^1\text{-}CH_3COO)(bpa)_2]^+$ ($[\mathbf{1}]^+$). Ellipsoids are drawn at the 40% probability level, and hydrogen atoms are omitted for clarity.

For the reaction of $[Rh_2(\mu\text{-}CH_3COO)_4(CH_3OH)_2]$ with a tridentate tpy, two coordination modes have been found.[47] One is a monodentate coordination at the *ax* sites of Rh−Rh bond through one of the outer pyridyl groups, as exemplified by **8** and **9**. The other one is a tridentate coordination at the *eq* planes, $[Rh_2(\mu\text{-}RCOO)(tpy)_2]^{3+}$ (R = CH_3,[47] C_6H_5[43]). The latter complexes were prepared by refluxing the mixture of $[Rh_2(\mu\text{-}RCOO)_4]$ and tpy in EtOH[47] or by stirring the acetonitrile solution of $[Rh_2(tpy)_2(CH_3CN)_4]^{4+}$ and $Bu_4N(C_6H_5CO_2)$.[43] Monodentate coordination occurs only through one of the peripheral pyridyl groups. Coordination of the central pyridyl nitrogen seems difficult due to the steric hindrance of peripheral pyridyl groups. The stepwise chelating reaction of $[Rh_2(\mu\text{-}CH_3COO)_4]$ with tpy or Cl-tpy was not observed at ambient temperature probably because of the destabilization of any intermediate species by steric hindrance.

Structures of the Dirhodium(II) Complexes. Steric structures of most of the complexes discussed in the previous section have been verified by the X-ray crystal structure analysis. Figure 1 shows the ORTEP drawing of the complex cation $[\mathbf{1}]^+$ ($[Rh_2(\mu\text{-}CH_3COO)_2(\eta^1\text{-}CH_3COO)(bpa)_2]^+$). The cation has an asymmetric structure with one of the two bpa ligands acting as a tridentate ligand occupying *ax-eq-eq* sites of one Rh atom (Rh2) and the other bpa functioning as a bidentate chelate at the *ax-eq* sites of another Rh atom (Rh1). One pyridyl group remains uncoordinated, and a monodentate acetate occupies one of the equatorial sites of Rh1. The complex cations $[\mathbf{2a}]^{2+}$ and $[\mathbf{2b}]^{2+}$ (Figures 2 and 3, respectively) are geometrical isomers of $[Rh_2(\mu\text{-}CH_3COO)_2(bpa)_2]^{2+}$. In each of them, two bpa ligands are equivalent

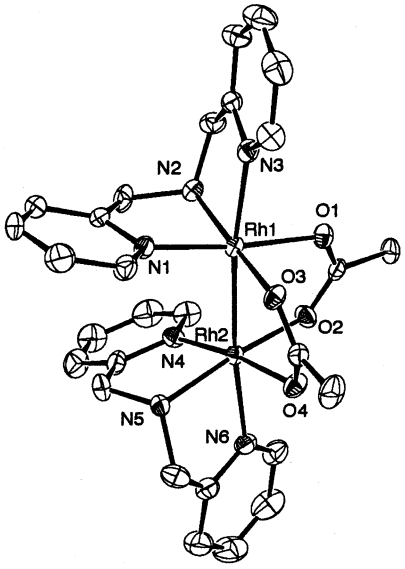

Figure 2. ORTEP drawing of C_2-$[Rh_2(\mu\text{-}CH_3COO)_2(bpa)_2]^{2+}$ ($[\mathbf{2a}]^{2+}$). Ellipsoids are drawn at the 50% probability level, and hydrogen atoms are omitted for clarity.

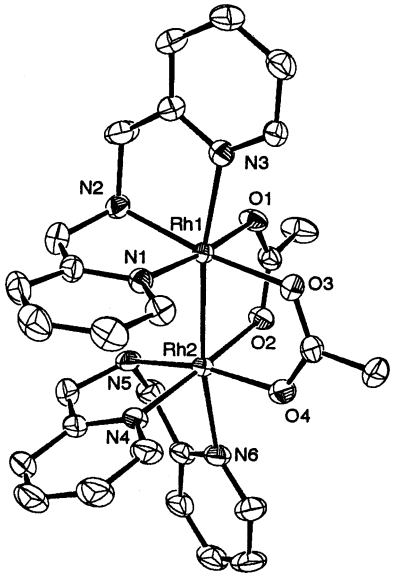

Figure 3. ORTEP drawing of C_s-$[Rh_2(\mu\text{-}CH_3COO)_2(bpa)_2]^{2+}$ ($[\mathbf{2b}]^{2+}$). Ellipsoids are drawn at the 50% probability level, and hydrogen atoms are omitted for clarity.

taking an *ax-eq-eq* tridentate mode. One of the pyridyl nitrogens coordinates to the *ax* site. The difference between the two cations is the relative steric arrangement of the two bpa chelates in the molecule. The complex cation $[\mathbf{2a}]^{2+}$ has approximate C_2 symmetry, while $[\mathbf{2b}]^{2+}$ has an idealized mirror plane normal to the Rh−Rh bond. Thus, $[\mathbf{2a}]^{2+}$ and $[\mathbf{2b}]^{2+}$ may be abbreviated as C_2 and C_s isomers, respectively, as already mentioned above.

The structures of the complex cations $[\mathbf{4}]^+$ ($[Rh_2(\mu\text{-}CH_3COO)_2(\eta^1\text{-}CH_3COO)(amp)_2]^+$) and $[\mathbf{6}]^{2+}$ ($[Rh_2(\mu\text{-}CH_3COO)_2(amp)_2(py)_2]^{2+}$) (Figure 4) have been reported in our previous communication.[50] The two amp ligands are not equivalent in $[\mathbf{4}]^+$. One of them forms a chelate ring at *ax-eq* positions of one of the rhodium ions (Rh1), while the other does at *eq-eq* sites of another rhodium atom (Rh2). A monodentate acetate ligand coordinates at the remaining *eq* site of Rh1

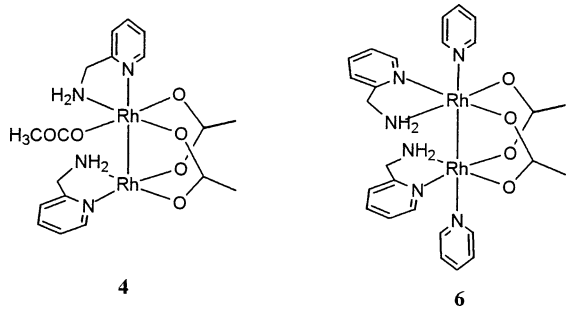

Figure 4. Molecular structure of $[\mathbf{4}]^+$ (left) and $[\mathbf{6}]^{2+}$ (right).

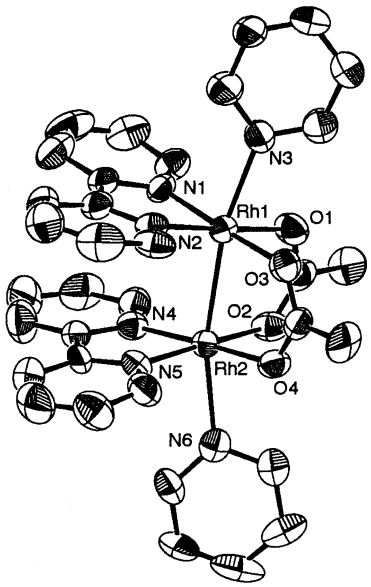

Figure 5. ORTEP drawing of $[Rh_2(\mu\text{-}CH_3COO)_2(bpy)_2(py)_2]^{2+}$ ($[\mathbf{7}]^{2+}$). Ellipsoids are drawn at the 50% probability level, and hydrogen atoms are omitted for clarity.

atom. The axial site of the Rh2 atom is only weakly coordinated by the oxygen (O2) of a bridging acetate of the neighboring dirhodium cation in the crystal (Rh−O, 2.599 Å). The two amp ligands are equivalent in the complex cation $[\mathbf{6}]^{2+}$ and form chelate rings at *eq-eq* sites, the rest of the equatorial sites and the axial positions being occupied by two bridging acetates and pyridine ligands, respectively.

The asymmetric unit of $[\mathbf{7}](PF_6)_2$ consists of two crystallographically independent dirhodium complex cations. The complex cation $[\mathbf{7}]^{2+}$ ($[Rh_2(\mu\text{-}CH_3COO)_2(bpy)_2(py)_2]^{2+}$) has an approximate C_{2v} symmetry and involves *eq-eq* chelates of bpy ligands (Figure 5).

The Rh−Rh distances for $[\mathbf{1}]^+$ (2.565(1) Å), $[\mathbf{2a}]^{2+}$ (2.568(1) Å), $[\mathbf{2b}]^{2+}$ (2.600(1) Å), $[\mathbf{4}]^+$ (2.5249(9) Å), $[\mathbf{6}]^{2+}$ (2.587(1), 2.585(1) Å), and $[\mathbf{7}]^{2+}$ (2.584(2), 2.593(2) Å) are very similar to one another and also to those of other $Rh_2(\mu\text{-}RCOO)_2$ complexes. Furthermore, overall structural features of the $Rh_2(\mu\text{-}CH_3COO)_2$ unit in these complexes are similar to those of other $Rh_2(\mu\text{-}RCOO)_2$ complexes.[1,41,43]

Figure 6 shows the perspective view of the Cl-tpy complex **9** ($[Rh_2(\mu\text{-}CH_3COO)_4(Cl\text{-}tpy)_2]$). The crystal structure of the tpy complex **8** was reported previously by Pruchnik et al.[47] We have also determined the structure of **8** independently. Interestingly, the space group of our crystals ($P\bar{1}$) is different from that in the previous report ($C2/c$). Nevertheless, the

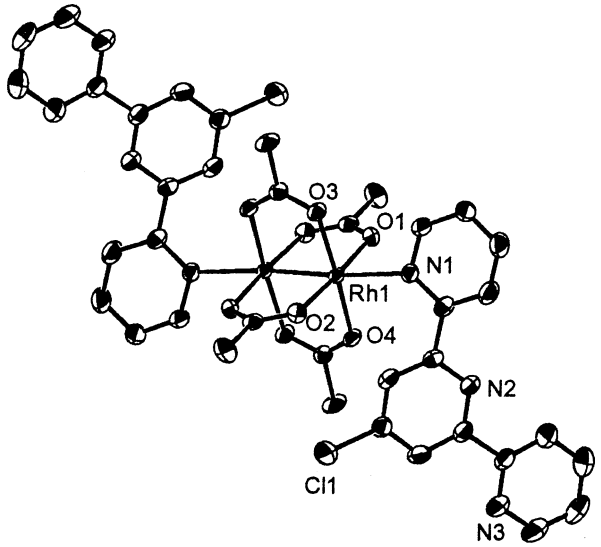

Figure 6. ORTEP drawing of $[Rh_2(\mu\text{-}CH_3COO)_4(Cl\text{-}tpy)_2]$ (**9**). Ellipsoids are drawn at the 50% probability level, and hydrogen atoms are omitted for clarity.

reported molecular structure of **8** is very similar to that of ours. Both **8** and **9** have a crystallographically imposed center of symmetry at the midpoint of the Rh−Rh single bond. In these complexes, tpy and Cl-tpy act as a monodentate ligand at the *ax* site by the coordination of one of the terminal pyridine rings. The Rh−Rh distances of **8** and **9** are 2.407-(1) and 2.4035(9) Å, respectively, which are shorter than those of other complexes mentioned above but in the range usually observed in $[Rh_2(\mu\text{-carboxylate})_4]$ complexes.

The axial Rh−N_{ax} (N: those of pyridine or pyridyl group) distances of our complexes span a fairly wide range from 2.111(6) to 2.354(5) Å. The distances may be classified into three groups. Typical Rh−N_{ax} bond lengths are found in $[\mathbf{6}]^{2+}$ (2.26 Å) and $[\mathbf{7}]^{2+}$ (2.24 Å). These values are close to the distances in, for example, $[Rh_2(\mu\text{-}CH_3COO)_2(CH_3CN)_4(py)_2](BF_4)_2$ (2.235 Å),[57] $[Rh_2(\mu\text{-}CH_3COO)_2(py)_6](CF_3SO_3)_2$ (2.234 Å),[58] and $[Rh_2(\mu\text{-}CH_3COO)_4(py)_2]$ (2.227(3) Å)[59] and may represent the distance without any significant steric requirement from the moieties at equatorial sites. Shorter Rh−N_{ax} distances found in the three compounds ($[\mathbf{1}]^+$ (2.218 Å), $[\mathbf{2a}]^{2+}$ (2.189 Å), and $[\mathbf{2b}]^{2+}$ (2.180 Å)) may be accounted for by the *ax*-*eq* chelate formation of the tridentate ligand. Similar short Rh−N_{ax} bonds are found in $[Rh_2(\mu\text{-}CH_3COO)_3(bpnp)]^+$ (bpnp = 2,7-bis(2-pyridyl)-1,8-naphthyridine) (2.195 Å)[60] and $[Rh_2(\mu\text{-}CH_3COO)_2(pynp)]^+$ (pynp = 2-(2-pyridyl)-1,8-naphthyridine) (2.204 Å),[9] where bpnp and pynp form *ax*-*eq* chelate rings. The shortest distance found in $[\mathbf{4}]^+$ (2.111(6) Å) may be regarded as an exceptional case, since the other *ax* site is only weakly coordinated (2.599(5) Å) by acetate oxygen of a neighboring dirhodium complex. The third group (**8** (2.322(2) Å) and **9** (2.354(5) Å)) has a longer Rh−N_{ax} distance probably due to steric repulsion between tpy or Cl-tpy ligand and bridging carboxylates.

A core structure similar to that for $[\mathbf{6}]^{2+}$ is proposed for $[\mathbf{5}]^{2+}$ on the basis of ^{1}H NMR (vide infra) and other analytical data. For insoluble pink solid **3**, a two-dimensional polymeric structure where the $Rh_2(CH_3COO)_4$ units are bridged by the bpa ligands is most likely, as has been considered for the insoluble solid $[Rh_2(\mu\text{-}CH_3COO)_4(amp)]_n$.

Other Properties of the Dirhodium(II) Complexes. (1) ^{1}H NMR Spectra. The two isomeric forms $[\mathbf{2a}]^{2+}$ and $[\mathbf{2b}]^{2+}$ are clearly distinguished by ^{1}H NMR spectra. While singlet acetate methyl signal was observed at 2.26 ppm for the C_2 isomer $[\mathbf{2a}]^{2+}$ in CD_2Cl_2, two methyl signals were found at 1.98 and 2.55 ppm for $[\mathbf{2b}]^{2+}$. The methylene signals of the bpa ligands of these complexes were observed in fairly wide range of magnetic field (2.56−4.77 ppm), reflecting various chemical circumstances around the methylene groups. One of the methylene protons of $[\mathbf{2a}]^{2+}$ appeared at significantly higher field (2.56 ppm) as compared with other methylene protons of $[\mathbf{2a}]^{2+}$ and all the methylene protons of $[\mathbf{2b}]^{2+}$. The steric structure of $[\mathbf{2a}]^{2+}$ shows that one of the methylene protons is located over the adjacent pyridyl ring coordinated to the opposite Rh atom in the molecule and should be under the influence of pyridyl ring current. A similar upfield shift was observed for $[\mathbf{6}]^{2+}$, which also has methylene groups over a pyridyl ring as verified by the X-ray structure.

The ^{1}H NMR spectrum of the asymmetric bpa complex $[\mathbf{1}]^+$ was complicated because of low symmetry of the complex. However, the observation of three sets of methyl signals from the acetate ligands at 1.00, 1.81, and 2.43 ppm as well as three sets of *o*-py signals at 8.75, 9.05, and 9.37 ppm both with integrated intensity ratio of 1:1:2 is consistent with the solid-state structure as verified by the X-ray diffraction. The ^{1}H NMR spectrum of asymmetric amp complex $[\mathbf{4}]^+$ at room temperature in D_2O showed two sets of amp and three acetate methyl signals as expected from the X-ray structure. For $[\mathbf{5}]^{2+}$ not only the amp signal patterns but also the chemical shifts in D_2O are similar to those of $[\mathbf{6}]^{2+}$ in CD_2Cl_2, where two amp ligands and two acetates are respectively equivalent. This observation suggests that $[\mathbf{5}]^{2+}$ also has a C_2 symmetry with the two amp ligands chelating at *eq* sites. ^{1}H NMR spectrum of the tpy complex **8** in acetone-d_6 coincided with the sum of the spectra of $[Rh_2(\mu\text{-}CH_3COO)_4]$ and the free ligand. A similar spectrum was observed for **9**. Thus, the axial ligands for **8** and **9** are dissociated in acetone.

(2) Electronic Spectra. As representative examples, the UV−vis spectra of $[\mathbf{1}]PF_6$, $[\mathbf{2a}](PF_6)_2$, $[\mathbf{2b}](PF_6)_2$, and $[\mathbf{6}](PF_6)_2$ in CH_2Cl_2 solutions are shown in Figure 7. Tetra- and dicarboxylate-bridged dirhodium(II) complexes are known to exhibit a visible band at around 450−600 nm. The band are assigned to the $\pi^* \rightarrow \sigma^*$ transition of the Rh−Rh bond.[1,2] It has been suggested that the transition energy depends significantly on the nature and the bond distances (to Rh) of axial ligands but not on the nature of equatorial

(57) Pimblett, G.; Garner, C. D.; Clegg, W. *J. Chem. Soc., Dalton Trans.* **1986**, 1257−1263.
(58) Dikareva, L. M.; Golubnichaya, M. A.; Baranovskii, I. B. *Russ. J. Inorg. Chem.* **1988**, *33*, 1179−1182.
(59) Christoph, G. G.; Koh, Y. B. *J. Am. Chem. Soc.* **1979**, *101*, 1422.
(60) Tikkanen, W. R.; Binamira-Soriaga, E.; Kaska, W. C.; Ford, P. C. *Inorg. Chem.* **1984**, *23*, 141−146.

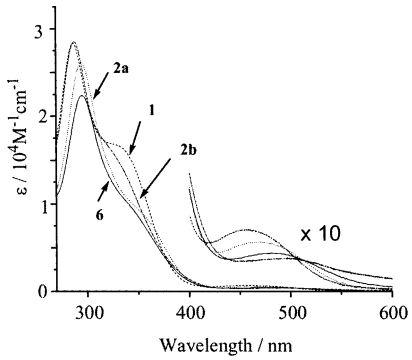

Figure 7. UV−vis absorption spectra of $[Rh_2(\mu\text{-}CH_3COO)_2(\eta^1\text{-}CH_3COO)(bpa)_2]PF_6$ ([**1**]PF$_6$, solid line), C_2-$[Rh_2(\mu\text{-}CH_3COO)_2(bpa)_2](PF_6)_2$ ([**2a**](PF$_6$)$_2$, dashed line), C_s-$[Rh_2(\mu\text{-}CH_3COO)_2(bpa)_2](PF_6)_2$ ([**2b**](PF$_6$)$_2$, dotted line), and $[Rh_2(\mu\text{-}CH_3COO)_2(amp)_2(py)_2](PF_6)_2$ ([**6**](PF$_6$)$_2$, dashed−dotted line) in CH_2Cl_2.

Table 3. Rh−N$_{ax}$(py) Bond Length (Å) and Electronic Absorption Peak Maximum of $\pi^*_{Rh-Rh} \rightarrow \sigma^*_{Rh-Rh}$ Transition for [**1**]$^+$, [**2a**]$^{2+}$, [**2b**]$^{2+}$, [**4**]$^+$, [**6**]$^{2+}$, [**7**]$^{2+}$, **8**, and **9**

		Rh−Rh$_{\pi^*\rightarrow\sigma^*}$	
	Rh−N$_{ax}$ dist	solid state	in CH_2Cl_2
[**1**]$^+$	2.183(8), 2.253(8) (av 2.218)		486
[**2a**]$^{2+}$	2.179(7), 2.198(7) (av 2.189)	454	456
[**2b**]$^{2+}$	2.157(4), 2.203(4) (av 2.180)		467
[**4**]$^{+\,a}$	2.111(6)		536^b
[**6**]$^{2+\,a}$	2.233(9)−2.281(9) (av 2.26)	495	508
[**7**]$^{2+}$	2.20(1)−2.27(1) (av 2.23)		
8	2.323(2)	561	
9	2.359(6)	561	

^{a} Reference 50. ^{b} In H_2O.

ones.[2,3,61] For example, the band maximum of $[Rh_2(\mu\text{-}CH_3COO)_4L_2]$ (L = H_2O, CH_3CN) is close to that of $[Rh_2(\mu\text{-}CH_2COO)_2(bpy\text{ or }phen)_2L_2]^{2+}$.[1,2,3,43] It is thus assumed that the different ligand combinations of the equatorial sites in $[Rh_2(\mu\text{-}CH_3COO)_4L_2]$ and $[Rh_2(\mu\text{-}CH_3COO)_2(amp)_2L_2]^{2+}$ do not give significant influence on the visible band energies. Since the axial ligands are often dissociated in solution, the visible band in the solid-state reflectance spectra (band maxima given in the Experimental Section) is discussed first by referring the crystal structural analyses. The Rh−N$_{ax}$ distances and the $\pi^* \rightarrow \sigma^*$ transition energies are summarized in Table 3. The visible bands of [**2a**](PF$_6$)$_2$ (Rh−N$_{ax}$ distance, average 2.189 Å), [**6**](PF$_6$)$_2$ (2.26 Å), and **9** (2.354 Å) were observed at 454, 508, and 561 nm, respectively. It is obvious that the absorption band shows a red shift with increasing Rh−N$_{ax}$ distances. Destabilization of the σ^* orbital may be less significant when the Rh−N$_{ax}$ distance is longer. In the case of asymmetric complex [**4**]ClO$_4$, the visible band (536 nm) is out of the energy range expected for the short Rh−N$_{ax}$ bond (2.111(6) Å). Influence of the short but sole Rh−N$_{ax}$ bond may be canceled out by the fairly long Rh−O distance of the opposite *ax* site. The reflectance spectrum of the polymer complex **3** exhibited the band at 534 nm, suggesting that the Rh−N$_{ax}$ distances would be around 2.3 Å.[1−3]

The electronic spectra of **8** and **9** in acetone are similar to each other and also similar to that of $[Rh_2(\mu\text{-}CH_3COO)_4]$ in acetone. The band at 603 nm in acetone is significantly red-shifted from that (561 nm) in the solid state for both **8** and **9**. The axial ligands must be liberated from the $Rh_2(CH_3COO)_4$ core in acetone, being consistent with the ^{1}H NMR measurements (vide supra). Addition of an excess amount of tpy or Cl-tpy to the corresponding acetone solution caused a significant blue shift of the band, suggesting the coordination of these ligands to the *ax* sites to some extent.

The $\pi^*-\sigma^*$ transition band in [**2a**](PF$_6$)$_2$ in solution (λ_{max} = 458 nm in CH_3CN, 456 nm in CH_2Cl_2) was observed in the region similar to that in the solid state (454 nm). The band of [**2b**](PF$_6$)$_2$ (467 nm in both CH_3CN and CH_2Cl_2) was also observed in the similar region. Thus, in the case of [**2a**](PF$_6$)$_2$ and [**2b**](PF$_6$)$_2$, the axial pyridyl nitrogens remain attached to the Rh atom in the solution. This may be due to the chelating effect incorporating with the *eq* donor groups. The lowest energy band in [**6**](PF$_6$)$_2$ was observed at 495 nm in CH_2Cl_2 which is close to the band maximum of the solid state (508 nm), suggesting that the axial pyridine ligands are retained in this solvent. However, the band shifted to 532 nm in acetonitrile, where the pyridine ligands may partially dissociate from the axial sites.

Complex [**5**](ClO$_4$)$_2$ was isolated in the form without axial ligands. The visible band in [**5**](ClO$_4$)$_2$ was observed at 577 nm in aqueous solution. The maximum is close to those (568 nm) in $[Rh_2(\mu\text{-}CH_3COO)_2(bpy\text{ or }phen)_2(H_2O)_2]$ in aqueous solution.[35] It is very likely that the axial sites of **5** are occupied by solvent water molecules.

Summary

Substitution-inert nature of the *eq* sites of the acetate-bridged dirhodium(II) center enabled us to isolate several intermediate species during the reaction of $[Rh_2(\mu\text{-}CH_3COO)_4(CH_3OH)_2]$ with bidentate amp and tridentate bpa. Different from the reactions with diphosphines,[28,29] these ligands coordinate only to one metal center as a chelating ligand. Bridging coordination has not been observed. The chelation process is preceded by the almost instantaneous coordination at the *ax* sites. The following steps involving *ax-eq* and then *eq-eq* chelate formation take days to complete at room temperature. The geometrical isomerism of the chelated complexes enables us to discuss further insight into the chelation mechanisms. The isolation of a series of dirhodium(II) complexes makes possible the systematic studies of the steric structures and electronic and ^{1}H NMR spectra.

Acknowledgment. Financial support from a Grant-in-Aid (No. 15036201) on Priority Area of "Reaction Control of Dynamic Complexes" from the Ministry of Education, Culture, Sports, Science, and Technology of Japan is gratefully acknowledged.

Supporting Information Available: X-ray crystallographic files in CIF format for the structure determinations of [**1**]PF$_6$·1.5H$_2$O, [**2a**](PF$_6$)$_2$, [**2b**](BF$_4$)$_2$, [**7**](PF$_6$)$_2$, **8**, and **9** and ORTEP diagrams of the complex cations [**4**]$^+$ and [**6**]$^{2+}$. This material is available free of charge via the Internet at http://pubs.acs.org.

IC030093W

(61) Handa, M.; Watanabe, M.; Yoshioka, D.; Kawabata, S.; Nukada, R.; Mikuriya, M.; Azuma, H.; Kasuga, K. *Bull. Chem. Soc. Jpn.* **1999**, *72*, 2681−2686.